

6. SITE 579¹

Shipboard Scientific Party²

HOLES 579, 579A

Date occupied: 1 June 1982 (579), 2–4 June (579A)

Date departed: 4 June 1982

Time on site: 2 days, 17 hr., 6 min.

Position (latitude, longitude): 38°37.68'N; 153°50.17'E (579)
38°37.61'N; 153°50.28'E (579A)

Water depth (sea level; corrected m, echo-sounding): 5736.6

Water depth (rig floor; corrected m, echo-sounding): 5746.6

Bottom felt (m, drill pipe): 5746.6 (579), 5755.0 (579A)

Penetration (m): 17.9, (579), 149.5 (579A)

Number of cores: 2 (579), 15 (579A)

Total length of cored section (m): 17.9 (579), 135.5 (579A)

Total core recovered (m): 16.90 (579), 115.87 (579A)

Core recovery (%): 94 (579), 86 (579A)

Oldest sediment cored:

Depth sub-bottom (m): 149.5

Nature: siliceous clay

Age: early Pliocene

Measured velocity (km/s): 1.5

Basement: Not reached

Principal results: A thick section of early Pliocene to Quaternary siliceous clay was recovered from two holes at Site 579. Siliceous microfossils (diatoms and radiolarians) are generally abundant and well preserved throughout much of the section. An interpretable and complete magnetic stratigraphy can be identified back to the middle of the Gilbert Reversed Epoch (early Pliocene).

One hundred and forty-nine meters of sediment were cored. Except for ash layers, the recovered sediments are relatively uniform in color being gray, dark gray, olive gray, and greenish gray. Although burrow mottles are abundant, the sediment lacks any depositional sedimentary structures. Based upon these data, the entire sedimentary section recovered at Site 579 is placed into one single lithologic unit. However, based upon variations in biogenic and inorganic sediment compounds, three subunits can be recog-

nized: a siliceous clay containing diatoms and radiolarians in approximately equal proportions, a clayey siliceous ooze with radiolarians somewhat more abundant than the diatoms, and a clayey diatom ooze.

The upper lithologic Subunit IA consists of 60 m of siliceous clay with 15–30% quartz. Twenty-seven ash layers and 83 thin, stiff, dark grayish green layers occur in this subunit. Subunit IB is a clayey siliceous ooze with 5–15% quartz and 5% or less disseminated volcanic glass. Twenty-four ash layers and 126 thin, indurated grayish green layers occur in this subunit. Lowermost lithologic Unit IC is approximately 46 m thick and contains from 3 to 25% quartz. There are only 10 ash layers in this subunit and 116 well-indurated dark grayish green layers.

Sedimentation rates are uniformly about 40 m/m.y., except for the interval near the Pliocene/Pleistocene boundary where the rates decrease to about 20 m/m.y.

Marginal weather prevented completion of the entire heat flow program. Measurements were not possible until Core 9. However, seven successful measurements were made between Cores 9 and 15 (~100–150 m sub-bottom depth). The temperature data clearly show a linear increase with depth. No temperature reversals were observed.

BACKGROUND AND OBJECTIVES

Site 579 (target Site NW-7A) lies near the southern margin of the transition zone between the subtropical and subarctic gyres. Because of its location, it forms an important link between the more siliceous, subarctic sites to the north and the calcareous-siliceous subtropical sites to the south. For this reason, it should record the most extreme southerly excursions of the subarctic front during the Neogene and Quaternary. When this information is combined with a study of the eolian input from the Asian mainland, a detailed paleoclimatic-paleoceanographic picture for this site should result.

Since this site is north of the abrupt thickening of the transparent acoustic layer, we may be able to learn something of the character of this layer.

Our specific scientific objectives were

1. To recover a detailed paleoceanographic record of the subtropical-subarctic transition zone for the late Neogene and Quaternary.
2. To establish a high-resolution midlatitude stratigraphy using paleomagnetism, tephrochronology, and biostratigraphy.
3. To determine the time of onset of significant biogenic silica accumulations for comparison with sites to the north and south.
4. To determine the late Cenozoic history of eolian input from the Asian mainland for comparison with the history of north-south migrations of the subarctic front.

OPERATIONS

After leaving Site 578, *Glomar Challenger* steamed northward to Site 579 (target Site NW-7A). Our passage was delayed somewhat due to strong head wind from a

¹ Heath, G. R., Burckle, L. H., et al., *Init. Repts. DSDP*, 86: Washington (U.S. Govt. Printing Office).

² Addresses: G. Ross Heath (Co-Chief Scientist) School of Oceanography, Oregon State University, Corvallis, OR 97331 (present address: College of Ocean and Fishery Sciences, University of Washington, Seattle, WA 98195); Lloyd H. Burckle (Co-Chief Scientist) Lamont-Doherty Geological Observatory, Palisades, NY 10964; Anthony E. D'Agostino, ARCO Exploration Company, Houston, TX 77056; Ulrich Bleil, Institut für Geophysik, Ruhr-Universität Bochum, D-4630 Bochum Querenburg, Federal Republic of Germany; Ki-iti Horai, Lamont-Doherty Geological Observatory, Palisades, NY 10964 (present address: Meteorological College, Chiba University, Chiba 277, Japan); Robert D. Jacobi, Department of Geological Sciences, SUNY Buffalo, Amherst, NY 14226; Tom Janacek, Department of Atmospheric & Oceanic Science, University of Michigan, Ann Arbor, MI 48109 (present address: Lamont-Doherty Geological Observatory, Palisades, NY 10964); Itaru Koizumi, College of General Education, Osaka University, Osaka 560, Japan; Lawrence A. Krissek, School of Oceanography, Oregon State University, Corvallis, OR 97331 (present address: Department of Geology and Mineralogy, Ohio State University, Columbus, OH 43210); Nicole Lenôtre, Bureau de Recherches Géologiques et Minières, Centre Océanologique de Bretagne, 45060 Orléans Cedex, France; Simonetta Monechi, Geological Research Division, Scripps Institution of Oceanography, La Jolla, CA 92093 (present address: Dipartimento di Scienze della Terra, Università di Firenze, 4 Via La Pira, 50121 Firenze, Italy); Joseph J. Morley, Lamont-Doherty Geological Observatory, Palisades, NY 10964; Peter Schultheiss, Institute of Oceanographic Sciences, Surrey GU8 5UB, United Kingdom; Audrey A. Wright, Deep Sea Drilling Project, Scripps Institution of Oceanography, La Jolla, CA 92093 (present address: Ocean Drilling Program, 500 University Drive West, Texas A&M University, College Station, TX 77843).

over the beacon. We immediately began running pipe and spudded in at 1428 hr. (0328Z). Two cores were recovered at Hole 579 before deteriorating weather forced us to pull clear of the mud line at 1920 hr. (0820Z) and insert heavy-wall joints. A gale which, at times, reached Force 7 prevented us from respudding the hole until 1625 hr. (0525Z), 2 June. This hole is now designated 579A. Taking advantage of a weather window, we completed coring at Hole 579A down to 149.5 m sub-bottom depth (Table 1).

Because of swell conditions, heat flow measurements were not made until we were well down in Hole 579A. The core nose unit operated successfully on each attempt, becoming a routine procedure. The heavy swell also affected core recovery. Unlike the previous Site 578, which had excellent recovery coupled with unusually calm weather, Site 579 experienced frequent heavy swells that resulted in sometimes distorted, stretched, or otherwise disturbed cores. Inserting extra shear pins seemed to help, but weather remained a factor in dictating good core recovery.

Due to increasingly poor recovery (2.37 m in Core 15) in well indurated clayey diatom ooze, coring was terminated and the drill string was retrieved. The ship was secured from its drilling mode at 1755 hr., 4 June, and proceeded north to Site 580 (target Site NW-5A).

LITHOSTRATIGRAPHY

The lithostratigraphy of sediments recovered at Site 579 was determined by visual inspection of the split cores and by smear slide analyses with a petrographic microscope. Except for ash layers, these sediments are relatively uniform in color, ranging from gray (5Y 5/1), dark gray (5Y 4/1), and olive gray (5Y 5/2 or 5Y 4/2) to greenish gray (5GY 5/1 or 5G 5/1). Mottles are abundant and range from faint to intense; the sediments lack depositional sedimentary structures. On the basis of these data, the entire sedimentary section recovered at Site

579 (Holes 579 and 579A) is classified as a single lithologic unit. However, this unit can be divided into three subunits based on the abundances of biogenic and inorganic sediment components determined from smear slide analyses (Fig. 1, Table 2). These three subunits are a siliceous clay (Subunit IA), a clayey siliceous ooze with radiolarians slightly more abundant than diatoms (Subunit IB), and a clayey diatom ooze (Subunit IC).

Volcanic ash layers are found throughout the entire sedimentary section, but they occur less frequently below Core 11 in Hole 579A. A total of 61 ash layers were identified. In addition, a large number (about 325) of thin (<0.5 cm), stiff to indurated, dark greenish gray (5G 4/1) layers were observed throughout the cores. Smear slide analysis of these layers showed no significant compositional difference from the adjacent "soft" sediments. Therefore, the genesis of these layers is unknown at this time. The distribution of ash layers with depth in Holes 579 and 579A is shown in Figure 1.

The three lithologic subunits are characterized as follows.

Subunit IA

This subunit is a siliceous clay that occurs in Core 579-1 and Section 579-2, CC (0.0–17.9 m sub-bottom), and in Sections 579A-1-1 through 579A-5-4 (14.0–60.0 m sub-bottom). It contains 15–30% quartz, 2–25% diatoms, and 0–15% radiolarians, with average values of approximately 20% quartz, 15% diatoms, and 7% radiolarians. Feldspar and volcanic glass abundances are each generally less than 5%; mica and heavy minerals, if present, have abundances of 2% or less. Clays form the remainder of the sediment, averaging approximately 45%. Twenty-seven ash layers and pockets occur in this subunit, with thicknesses ranging from 2 to 19 cm. Eighty-three of the thin, stiff, dark grayish-green layers occur within this interval.

Subunit IB

This subunit is a clayey siliceous ooze that occurs in Sections 579A-5-5 through 579A-10-2 (60.0–102.5 m sub-bottom). It contains 5–15% quartz, 4–30% diatoms, and 13–35% radiolarians, with average values of approximately 10% quartz, 20% diatoms, and 22% radiolarians. Disseminated volcanic glass abundances are generally 5% or less, and feldspar forms 2% or less of the sediments. Heavy minerals, when present, occur only in trace amounts. The remainder of the sediment, averaging approximately 40%, is composed of clays. Twenty-four ash layers and pockets and 126 of the thin, stiff, dark grayish green layers occur within this interval. The ash layers range in thickness from 1.5 to 13.0 cm.

Subunit IC

This subunit is a clayey diatom ooze that occurs in Sections 579A-10-3 through 579A-15, CC (102.5–149.5 m sub-bottom). It contains 3–25% quartz, 25–60% diatoms, and 2–30% radiolarians, with average values of approximately 10% quartz, 40% diatoms, and 8% radiolarians. Volcanic glass and feldspar abundances are generally 2–5%; heavy minerals, when present, occur only

Table 1. Site 579 coring summary.

Core	Date (June, 1982)	Local time	Depth from drill floor (m)	Depth below seafloor (m)	Length cored (m)	Length recovered (m)	Percent recovered
Hole 579							
1	1	1625	5746.6–5755.0	0.0–8.4	8.4	8.44	100
2	1	1845	5755.0–5764.5	8.4–17.9	9.5	8.46	89
					17.9	16.90	94
Hole 579A							
1	2	1832	5760.6–5770.1	14.0–23.5	9.5	9.30	98
2	2	2045	5770.1–5779.6	23.5–33.0	9.5	9.70	102
3	2	2310	5779.6–5789.1	33.0–42.5	9.5	8.88	93
4	3	0137	5789.1–5798.6	42.5–52.0	9.5	5.36	56
5	3	0400	5798.6–5808.1	52.0–61.5	9.5	9.03	95
6	3	0630	5808.1–5817.6	61.5–71.0	9.5	7.94	84
7	3	0855	5817.6–5827.1	71.0–80.5	9.5	8.27	87
8	3	1105	5827.1–5836.6	80.5–90.0	9.5	9.66	102
9	3	1335	5836.6–5846.1	90.0–99.5	9.5	7.68	81
10	3	1620	5846.1–5855.6	99.5–109.0	9.5	7.59	80
11	3	1840	5855.6–5865.1	109.0–118.5	9.5	7.30	77
12	3	2116	5865.1–5874.5	118.5–128.0	9.5	8.34	88
13	4	0015	5874.5–5884.1	128.0–137.5	9.5	6.95	73
14	4	0250	5884.1–5893.6	137.5–147.0	9.5	7.50	79
15	4	0510	5893.6–5896.1	147.0–149.5	2.5	2.37	95
					135.5	115.87	86
					(total)	(total)	(avg.)

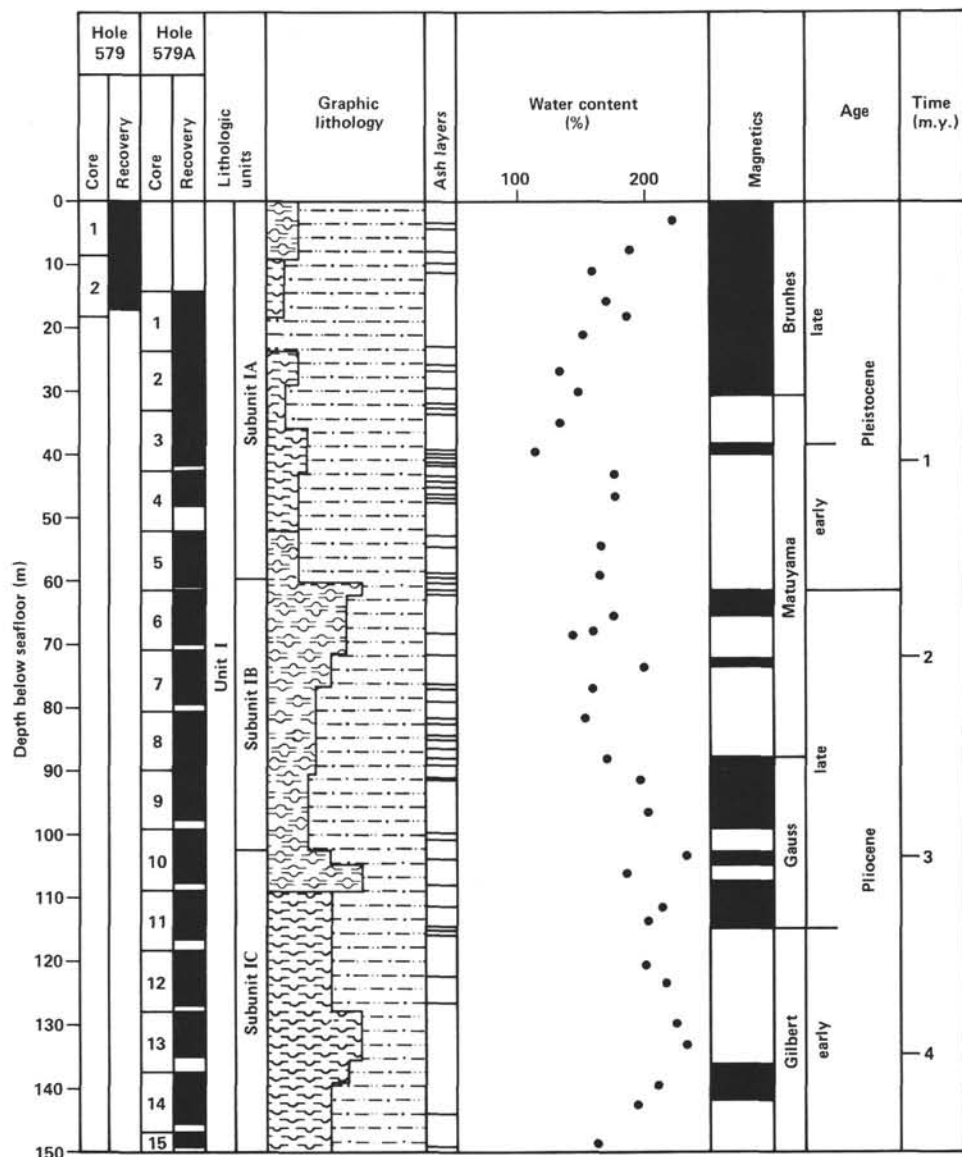


Figure 1. Site summary diagram showing Site 579 core numbers, core recovery, lithologic units, graphic lithology, ash layer locations, water content (%), magnetostratigraphy, and ages. Symbols used in graphic lithology column are defined in Introduction and Explanatory Notes (this volume).

Table 2. Site 579 lithostratigraphic units.

Lithologic unit	Cored interval		Sub-bottom depth (m)	Composition (%)		
	Hole 579	Hole 579A		Quartz	Diatom	Radiolarians
I: Siliceous clay						
Subunit IA: Siliceous clay	1-1, 0 cm to 2,CC	1-1, 0 cm to 5-4, 150 cm	0.0-60.0	15-30	2-25	0-15
Subunit IB: Clayey siliceous ooze		5-5, 0 cm to 10-2, 150 cm	60.0-102.5	5-15	4-30	13-35
Subunit IC: Clayey diatom ooze		10-3, 0 cm to 15,CC	102.5-149.5	3-25	25-60	2-30

frontal passage. On 1 June, shortly after midnight (0006 hr. local time, 1306Z), the beacon was dropped over the drill site, gear was retrieved, and the ship positioned in trace amounts. The remainder of the sediments, averaging approximately 38%, is composed of clays. Ten ash layers and pockets and 116 of the thin, stiff, dark gray-

ish green occur within this interval. The ash layers range in thickness from 3 to 11 cm.

SEISMIC CORRELATIONS

High resolution seismic reflection profiles (3.5 and 12 kHz) and 100-Hz reflection profiles were recorded at Site

579. Only a hull-mounted 3.5-kHz sound source was utilized. The 3.5-kHz echograms over Site 579 reveal a fairly uniform seismic section of parallel sub-bottom reflectors (Fig. 2). This seismic section can be divided into a four-part sequence based primarily on gaps in the reflector sequence (Table 3).

The uppermost seismic unit (seismic Unit 1) consists of strong reflectors and extends to 0.0268 s below the seafloor (20.3 m at 1513 m/s; 19.0 m at 1420 m/s). A thin transparent layer below the deepest reflector in seismic Unit 1 differentiates it from the top of seismic Unit 2. Seismic Unit 2 consists of three strong reflectors and extends to 0.0459 s below the seafloor (34.7 m at 1513 m/s; 32.6 m at 1420 m/s). A thin transparent layer at the base of seismic Unit 2 distinguishes it from the top of seismic Unit 3. Seismic Unit 3 consists of five intermediate-strong reflectors and extends to 0.0654 s below the seafloor (49.4 m at 1513 m/s; 46.4 m at 1420 m/s). Seismic Unit 4 consists of generally weak and discontinuous reflectors; only the top reflector is of intermediate strength. It extends to 0.0945 s below the seafloor (71.4 m at 1513 m/s; 67.1 m at 1420 m/s).

Identifying the source of these reflectors proved to be especially difficult at this site for two major reasons: (1) The moderate to heavy seas during the coring operation resulted in cores with a relatively high percentage of discrete "flow-in" zones. The uncertainty in the possible depths of most ashes because of this "flow-in" is quite large (up to 3 m). (2) A large number of equally strong

and closely spaced reflectors occurs in the upper 70 m of the sediment section. The range of possible velocities results in a range of computed depths for most reflectors that overlaps with the depths of the adjacent reflectors. The combination of unknown depths for both seismic reflectors and lithologic units results in particularly difficult correlations. The seismically transparent layers, the variable strength of reflection signals, and the precise depths of some lithologic units do, however, allow some relatively reliable correlations (i. e., Reflectors 1b, 1e, 1f, 3a, 3d, 3d', 4b, 4d, and 4e; Table 3). As at Site 578, the seismically transparent layers correlate with lithologic sections that lack ash layers. No such correlation is observed with the thin, pyritic, dark green layers which have anomalously high velocities like those of the ash layers. The source of the reflectors appears to be ash layers (Table 3).

Based on the proposed correlations, the top of seismic Unit 2 is probably the ash layer observed in Sample 579A-1-6, 66-75 cm (ash #3). The top of seismic Unit 3 is the ash layer located in Sample 579A-2-6, 106-129 cm (ash #8). The top of seismic Unit 4 may be located in Sample 579A-4-3, 55-60 cm (ash #15). Seismic Unit 4 may extend to ash #22 in Sample 579A-6-5, 59.5-67 cm. The top of lithologic Subunit IB may be associated with seismic Reflector 4c'.

The 100-Hz seismic reflection profiles reveal a four-part seismic section at Site 579 (Fig. 3). The uppermost seismic unit (Unit 1) extends to about 0.12 s below the

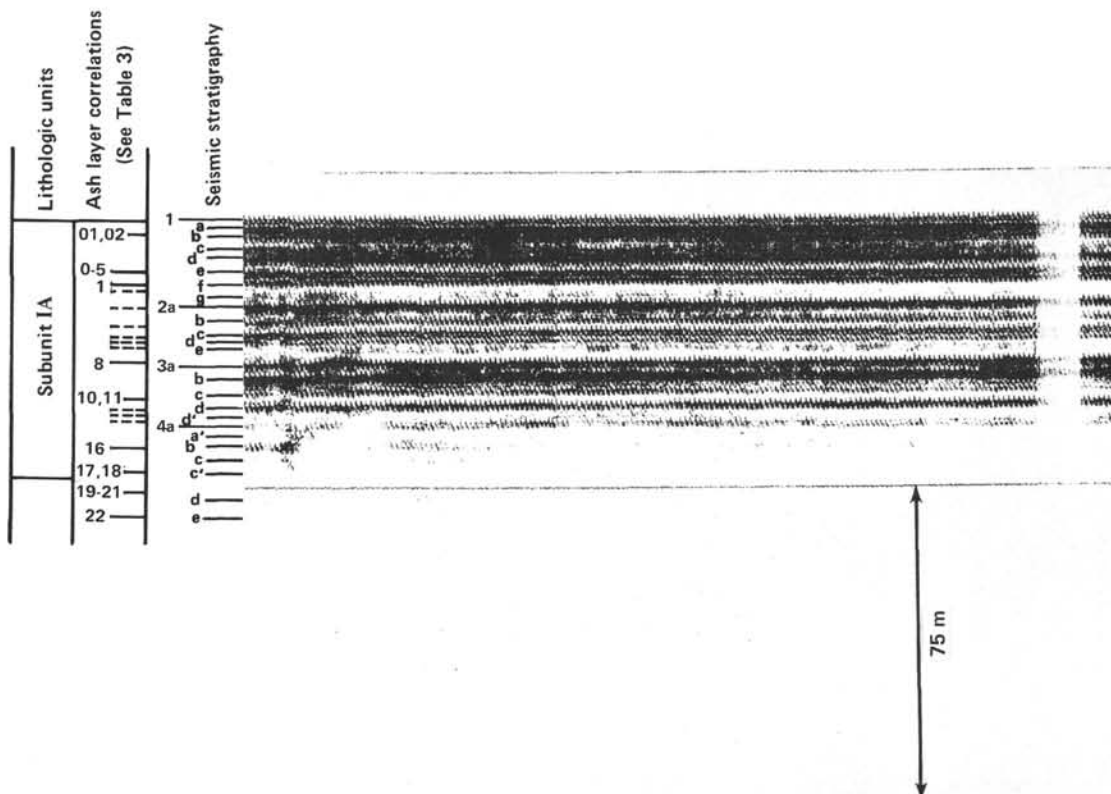


Figure 2. 3.5-kHz echogram near Site 579 showing the four-part seismic sequence described in the text. Lithostratigraphic correlations made assuming a velocity of 1480 m/s.

Table 3. 3.5-kHz seismic correlations, Site 579.

Reflector	Relative strength ^a	Depth below seafloor (s)	Depth below seafloor (m)		Depth in core (m)		Source
			1513 m/s	1420 m/s	Observed	Corrected for possible "flow-in"	
1a	I	0.00310	2.34				
1b	I-S	0.00569	4.31	3.95	3.35		Ash 01
1c	W-S	0.00886	6.7	6.29	3.6		Ash 02
1d	VS	0.0124	9.35	8.78			
1e	S	0.0169	12.78	12.00	11.7		Ash 0-5
1f	S-VS	0.020	15.12	14.2	14.7		Ash 1
1g	IT-W	0.0241	18.24	17.13	16.1		Ash 2?
2a	VS	0.0268- 0.0279	20.26- 21.04	19.03- 19.76	22.8	19.8	Ash 3?
2b	S	0.0319	24.08	22.61	25.7-26.4	24.7-25.4	Ash 4?
2c	S	0.0360	27.20	25.54	29.15	27.1	Ash 5?
2d	IT-W	0.0386	29.15	27.38	31.6	28.6	Ash 6??
2e	IT-W	0.0400- 0.0412	30.24- 31.18	28.4- 29.28	31.9	28.9	Ash 7??
3a	S	0.0459	34.71	32.60	32.4	29.4	Ash 8
3b	VS	0.0503	38.03	35.72	39.75	37.25	Ash 9?
3c	S	0.0552	41.77	39.23	40.75	38.25	Ash 10, 11?
3d	S	0.0594	44.89	42.16	43.9	No flow-in	Ash 12
3d'	IT	0.0619	46.76	43.92	45.1	No flow-in	Ash 14
4a	I	0.0654	49.41	46.40	46.3	No flow-in	Ash 15?
4a'	IT	0.0682	51.60	48.46	Missing section		Missing section
4b	W-I	0.0711	53.78	50.51	52.4	No flow-in above ash	Ash 16
4c	IT-W	0.0742- 0.0752	56.12- 56.82	52.70- 53.36	58.25 58.85	53.29 53.85	Ash 17, 18??
[4c'	IT	0.0784	59.31	55.70]	Missing section		from flow-in
4d	IT	0.0880	66.56	62.51	62.25- 62.6- 62.75	No flow-in above ash	Ash 19 Ash 20 Ash 21
4e	IT	0.0945	71.44	67.09	68.1		Ash 22

^a IT = intermittent, weak; W = weak, but generally continuous; I = intermediate; S = strong; VS = very strong.

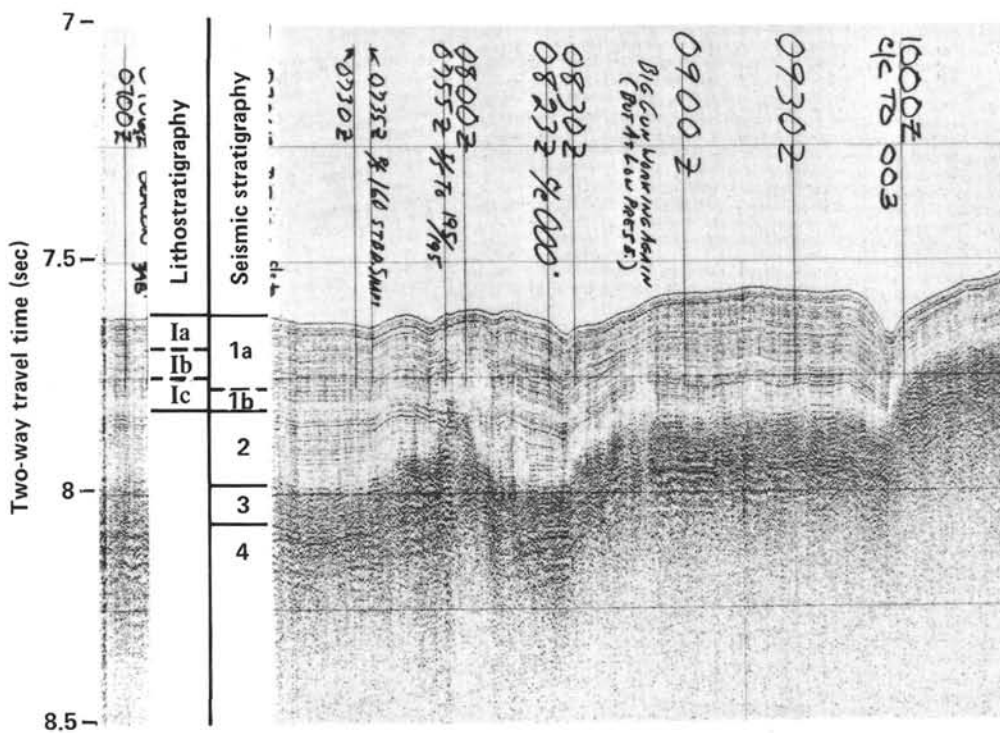


Figure 3. 100-Hz reflection profile over Site 579 showing the four-part seismic sequence described in the text.

seafloor (90 m, 1500 m/s) and consists of two subunits. The upper seismic subunit (Subunit 1a) is composed of strong, parallel, and continuous reflectors and extends to about 0.1 s below the seafloor (75 m at 1500 m/s). Seismic Subunit 1b occurs between 0.1 and 0.12 s (75 and 90 m at 1500 m/s) and consists of weak, discontinuous reflectors and transparent zones. The base of seismic Unit 1 is fairly close to the base of lithostratigraphic Subunit IB, at 102.5 m below the seafloor.

Seismic Unit 2 consists of strong, continuous, parallel reflectors to about 0.18 s below the seafloor (135 m at 1500 m/s) and a slightly transparent zone with weak, discontinuous echos to about 0.21 s below the seafloor (157.5 m at 1500 m/s). Seismic Unit 3 consists of strong, incoherent echos that extend to 0.27 s below the seafloor. Seismic Unit 3 probably represents Cretaceous chert and associated sedimentary rocks. Seismic Unit 4 con-

sists of a very strong, prolonged echo and probably is basalt basement.

BIOSTRATIGRAPHY

At Site 579 we cored 149.5 m of late Quaternary through early Pliocene sediment. No calcareous microfossils were found in any of the core catcher samples from the two holes taken at this site. Abundant, well preserved diatoms were found in all Pleistocene samples except for Sample 579A-4,CC where they were only moderately well preserved. Specimens in the early Pliocene were only moderately to poorly preserved. The shipboard diatom and radiolarian analyses did not detect any major hiatuses in the interval cored. A preliminary shipboard analysis of the moderately to well preserved silicoflagellates in samples from Hole 579A was also made (see Bukry and Monechi, this volume).

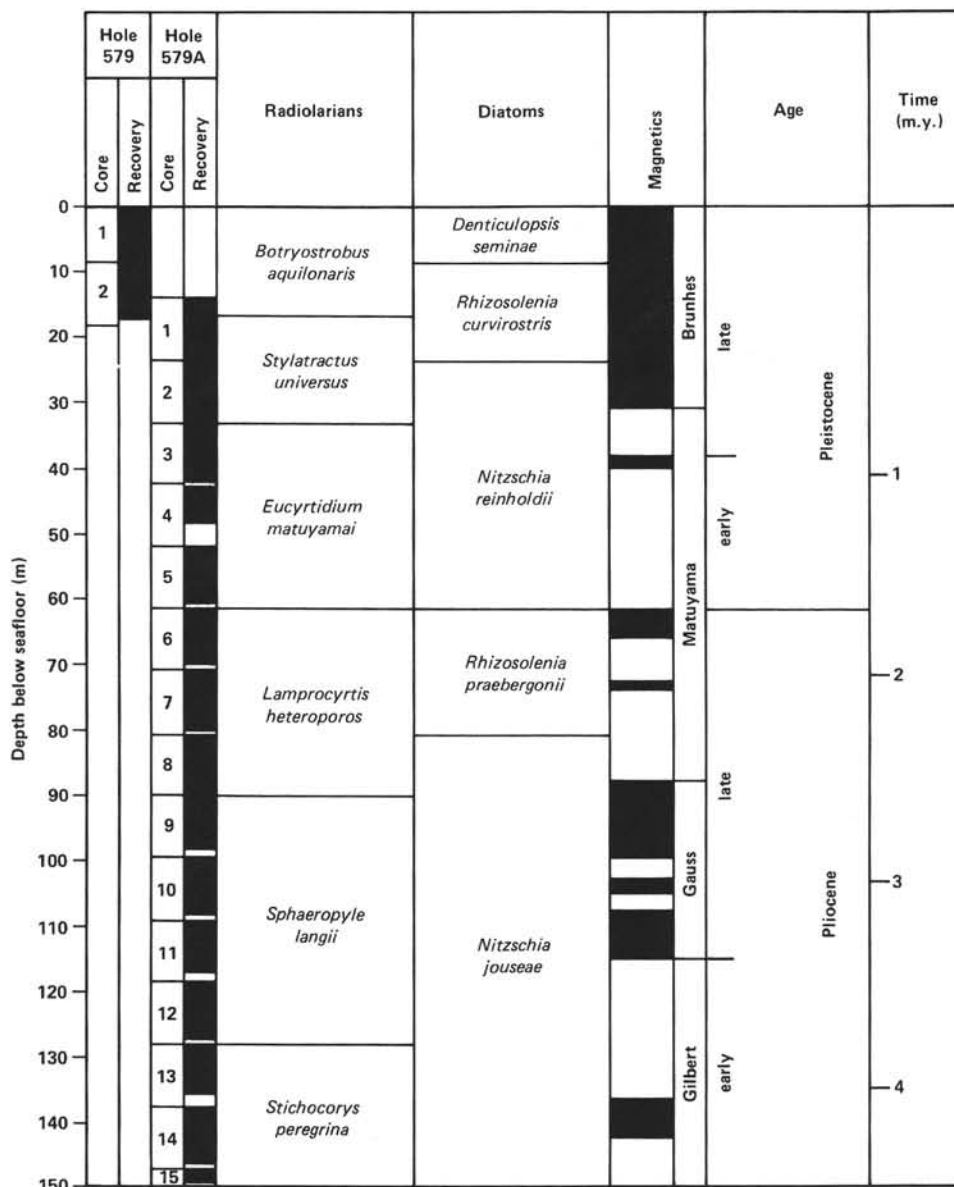


Figure 4. Site 579 biostratigraphic and magnetostratigraphic summary.

The diatom and radiolarian biostratigraphy is shown in summary form in Figure 4. According to this stratigraphy, the boundary between early and late Pleistocene falls within Core 579A-3. The Pliocene/Pleistocene boundary occurs in Core 579A-6.

Nannofossils

No calcareous nannofossils were found in any of the cores recovered at Site 579.

Planktonic Foraminifers

Seventeen core-catcher samples from two holes (579 and 579A) were examined. Hole 579 consisted of only two cores, and both core-catcher samples were barren of foraminifers. All 15 samples from Hole 579A were also barren of any foraminifers.

Radiolarians

Late Quaternary through early Pliocene radiolarians occur in sediment samples from Site 579 (Holes 579 and 579A). The preliminary radiolarian biostratigraphy for each of these holes is shown in Figure 4.

The entire sediment sequence from Hole 579 is late Quaternary in age containing an abundant, well preserved radiolarian fauna characteristic of the *Botryostrobus aquilonaris* Zone (Hays, 1970). The absence of *Lychnocanoma grande* in the first section (Sample 579-1-1, 2-3 cm) indicates that the sediments at the top of Hole 579 are less than 50,000 yr. old. In the core-catcher sample from Core 2, the presence of *Stylatractus universus* places this faunal assemblage within the *S. universus* Zone (Hays, 1970).

Radiolarians were present in all core catcher samples from Hole 579A, ranging in age from late Quaternary (Sample 579A-1,CC) through early Pliocene (Sample 579A-15,CC). Samples 579A-1,CC and 579A-2,CC contained an abundant, well preserved radiolarian fauna characteristic of the late Quaternary *S. universus* Zone (Hays, 1970). The top of Sample 579A-1-1, 5-7 cm did not contain *S. universus* and was assigned to the *B. aquilonaris* Zone. Comparing these results with those from Hole 579, it would appear that the base of the *B. aquilonaris* Zone (Hays, 1970) occurs somewhere in the middle of Core 579A-1. Radiolarians in Samples 579A-3,CC through 579A-6,CC were abundant and well preserved, except for Sample 579A-4,CC where preservation was only moderate. The presence of *Eucyrtidium matuyamai* in the core-catcher samples from Cores 3 through 5 indicates that the sediment sequence is early Pleistocene in age (*E. matuyamai* Zone [Hays, 1970; Foreman, 1973]) with the Pliocene/Pleistocene boundary occurring in the upper portion of Core 6. The abundant, well-preserved radiolarian fauna in Samples 579A-6,CC through 579A-8,CC did not contain *E. matuyamai* or *Stichocorys peregrina*, indicating that this sediment sequence is late Pliocene in age (*Lamprocyrtis heteroporos* Zone [Hays, 1970; Foreman, 1975]). The *Sphaeropyle langii* Zone (Foreman, 1975), based on the presence of *Stichocorys peregrina* and *Sphaeropyle langii*, extends from Cores 9 through 12. The boundary between late and early Pliocene is located within Core 11. The absence of *S. langii*, *Didymocyrtis penultima*, and *Diartus hughesi* in the fauna from

Samples 579A-13,CC through 579A-15,CC places this sediment sequence in the early Pliocene *Stichocorys peregrina* Zone (Riedel and Sanfilippo, 1970; Foreman, 1975).

Diatoms

Early Pliocene to Pleistocene diatoms occur in Holes 579 and 579A. Six diatom zones were observed in Holes 579 and 579A. The assemblages alternate between a dominance of warm water species and cold water species. Diatoms are abundant to common and well preserved.

Core 579-1 belongs to the latest Quaternary *Denticulopsis seminae* Zone (Koizumi, 1973). Cores 579-2 and 579A-1 are assigned to the late Quaternary *Rhizosolenia curvirostris* Zone. The base of this zone is tentatively defined by the last occurrence of *Nitzschia reinholdii*. Diatom assemblages in Cores 579A-2 through 579A-5 are placed in the *N. reinholdii* Zone. The last occurrence of the silicoflagellate *Mesocena quadrangula* in Core 2 indicates this sample is placed around the Jaramillo Event of the Matuyama Epoch. Cores 6 and 7 are correlated with the late Pliocene *R. praebregonii* Zone. The Pliocene/Pleistocene boundary, therefore, is placed somewhere within Core 6. The middle to early Pliocene *N. jouseae* Zone occurs in Cores 8 through 15. Core 8 is placed in the upper part of the Gauss Epoch by the co-occurrence of *R. praebregonii* and *Cussia tatsunokuchensis*. Core 12 is placed in the middle part of the Gilbert Epoch by the presence of *Cosmiodiscus insignis*. These two diatom events argue for correlation with the lower part of the *N. jouseae* Zone (early Pliocene) in Cores 12 through 13.

PALEOMAGNETICS

Paleomagnetic determinations were made on a total of 298 samples from the sediment cores recovered at the two holes drilled at Site 579. The results are briefly summarized here and documented in detail in a separate report (see Bleil, this volume).

The intensity of the natural remanent magnetization (NRM) is highly variable throughout the entire section recovered (varying from about 2×10^{-7} to about 5×10^{-5} emu/cm³). There is no consistent downhole trend in the NRM intensities. However, higher values are generally observed for normally polarized samples, indicating the presence of at least some overprinting by viscous components. With but a few exceptions, the magnetic stability was high; median destructive field (MDF) measurements typically yielded values of 300 ± 50 Oe. Lower MDF values and related larger directional changes of the magnetization directions upon AF demagnetization were more frequent in core sections showing clear evidence of drilling disturbance.

The polarity pattern derived from the stable magnetization directions is shown in Figure 4. In some cases, the quality of the reversal chronology is limited by incomplete recovery or badly disturbed zones. The two cores recovered from Hole 579 acquired their remanent magnetization during the present normal geomagnetic Brunhes Epoch. Therefore the sediments at the base of this hole (17.9 m) are younger than 0.73 m.y. An almost complete reversal sequence for the last 4.5 m.y. was ob-

tained in Hole 579A. The Brunhes/Matuyama boundary was recognized at a sub-bottom depth of 30.65 m (Sample 579A-2-5, 115 cm), the Jaramillo Event between 38.65 and 39.85 m (Samples 579A-3-4, 115 cm to 579A-3-5, 85 cm), indicating an average sedimentation rate of about 40.7 m/m.y. for the last 1 m.y. The Olduvai and one of the Reunion events can be identified in the older part of the Matuyama Epoch. The Matuyama/Gauss boundary was identified at 87.95 m sub-bottom (Sample 579A-8-5, 145 cm). Both the Kaena and Mammoth events are present, indicating that the geomagnetic record is also continuous and complete during the normal geomagnetic Gauss Epoch. The deepest clearly identifiable magnetic boundary at this site is the Gauss/Gilbert transition at about 115.01 m sub-bottom (Sample 579A-11-5, 1 cm). Between this depth and the base of the hole the paleomagnetic measurements revealed only one additional zone of positive polarity (136.38 to 141.95 m sub-bottom; Samples 579A-13-5, 88 cm to 579A-14-3, 145 cm). Assuming that no drastic increase in accumulation rate occurred at this level, the interval has been identified as the Nunivak Event. The youngest normal event in the Gilbert Epoch, the Cochiti, apparently lies in the 2.5-m gap between the base of Core 13 and the top of Core 14.

On the basis of the most recent polarity time scale of Berggren et al. (in press), the extrapolated absolute age of the base of Hole 579A is no more than 4.40 m.y. The average accumulation rate over the period of time represented by the entire sedimentary sequence at Site 579 thus was about 30.8 m/m.y. Compared to the other sites drilled on Leg 86, sedimentation rates at Site 579 were more variable, apparently due to real fluctuations in the supply of sediment.

SEDIMENT ACCUMULATION RATES

Paleomagnetic reversal boundaries were used to calculate the sedimentation rate at Site 579. According to the age–depth plot (Fig. 5) for this site, the sedimentation rate for the late Quaternary averages about 40 m/m.y. This rate decreases to approximately 20 m/m.y. near the Pliocene/Pleistocene boundary, but the rate increases again to 40 m/m.y. during the late early and late Pliocene. Changes in sedimentation rate do not appear to be related to lithologic type.

PHYSICAL PROPERTIES

Physical properties measurements at Site 579 were performed using mainly standard Deep Sea Drilling Project (DSDP) methods (Boyce, 1976a, b; see Introduction and Explanatory Notes, this volume). Table 4 summarizes the properties measured at Holes 579 and 579A. Measurements were taken at approximately 4.5-m intervals throughout the core. Figures 6, 7, and 8 show profiles of compressional and shear wave velocity, shear strength, and saturated bulk density and water content, respectively. A full discussion of the physical properties of the recovered sediments is given by Schultheiss (this volume), but some of the more interesting features are highlighted here:

1. The compressional wave velocity profile is dominated by many (61) high velocity ash layers and numer-

ous (~325) thin (<0.5 cm), stiff to indurated dark greenish gray layers. Velocities measured in a few ash layers are typically about 1600 m/s. The thin indurated green layers also have higher velocities but they tend to be variable, one was as high as 1770 m/s. Velocities in the siliceous clay and ooze are remarkably uniform throughout the site at 1480 m/s (Fig. 6).

2. Shear wave velocity measurements show no distinct trends down to 73 m sub-bottom depth (Fig. 6). The transducer broke at this point, preventing further measurements.

3. Shear strength measurements (Fig. 7), although exhibiting a large amount of scatter, show increasing strength down the hole. A major discontinuity exists in Section 579A-9-5, with very high shear strengths relative to shallower sections. Values decrease again in Core 579A-10, however. This maximum cannot be explained by any visible lithological changes.

4. A good example of “flow-in” is found in the bottom of Core 579A-6-5 (Fig. 7). Measurements with both the hand-held and motorized vane showed that the remolded flow-in section had decreased in strength by a factor of about four from 380 g/cm² in the “undisturbed” region to 100 g/cm² in the section containing “flow-in.”

5. The water-content profile (Fig. 8) can be split into three units. Unit I (from 0 to 41 m sub-bottom depth) has a decreasing water content from 220 to 111%, which is probably caused by normal consolidation processes. Unit II (from 41 to 134 m sub-bottom depth) has slowly increasing water content from around 170 to 228%, with a rapid change occurring at the boundary between Units I and II. Unit III, below 134 m sub-bottom depth, shows a decreasing water content down to 158% at 149 m sub-bottom.

These units do not correlate with the lithological units based on visual descriptions. It is probable that changes in clay mineralogy are responsible for the strength variations observed.

INORGANIC GEOCHEMISTRY

Five squeezed core samples, one from Hole 579 and four from Hole 579A, were analyzed for the standard suite of components: pH, alkalinity, salinity, calcium, magnesium, and chlorinity (Table 5). No *in situ* samples were taken.

Calcium increases linearly with depth (Fig. 9), suggesting diffusion between a source below the drilled section (presumably carbonate associated with the strong chert reflector) and the sink formed by the overlying ocean waters. Magnesium decreases through the cored interval, probably due to the formation of smectite by alteration of the abundant volcanic ash in the section. The slight initial increase in alkalinity may reflect sulfate reduction (to oxidize organic matter), but the trend reverses below 60 m, again probably because of ash alteration.

HEAT FLOW

Bad weather prevented the collection of a full profile of downhole temperature measurements by the new Woods Hole Oceanographic Institution (WHOI) heat flow instrument at this site. Heat flow measurements were not

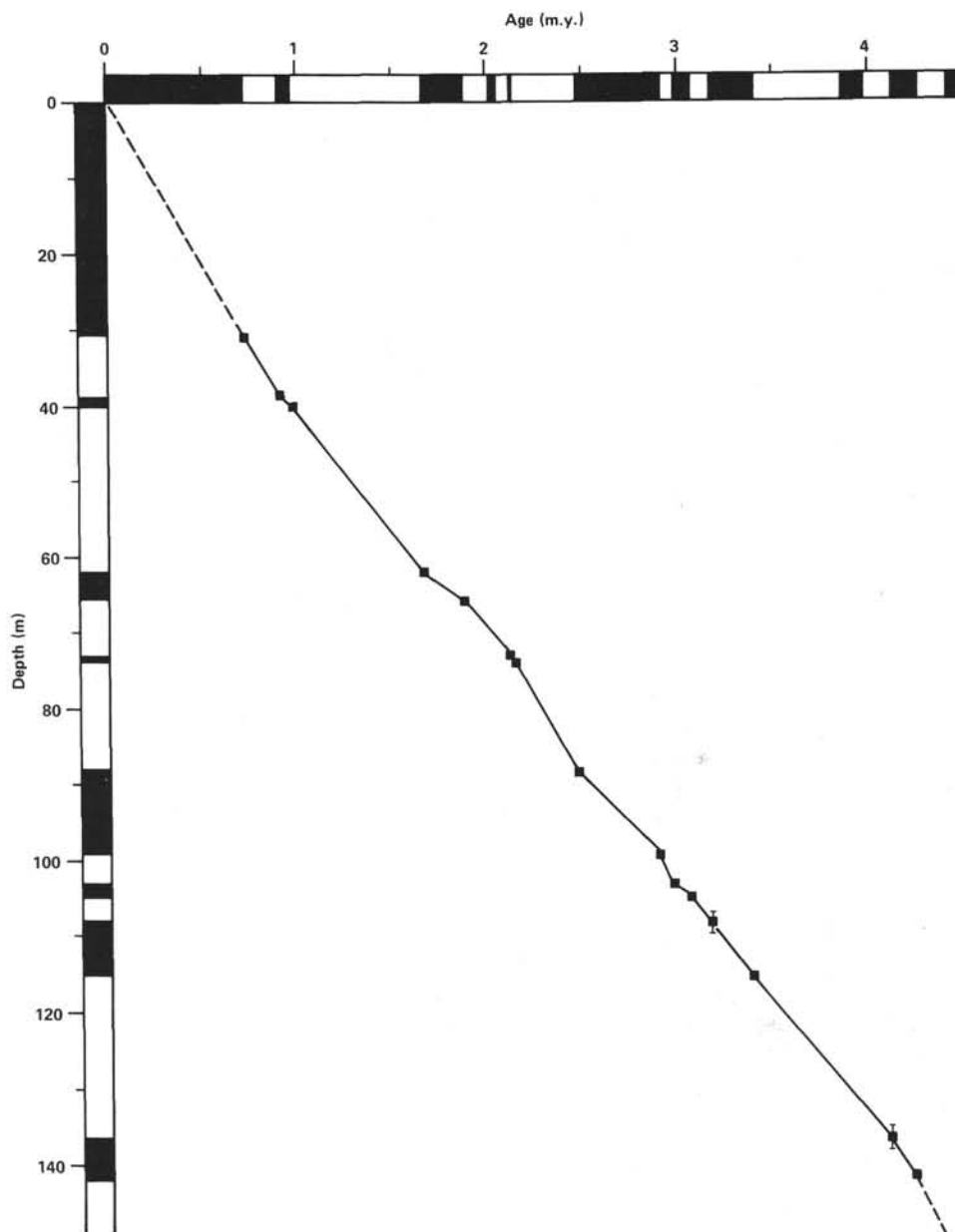


Figure 5. Site 579 sediment accumulation rates derived from the paleomagnetic reversal record.

Table 4. Physical properties measurements made at Site 579.

Physical property	Holes 579 and 579A
Shear strength:	
Hand-operated vane	x
Motorized vane	x
Wave velocity:	
Shear wave	x
Compressional wave	x
Water content/bulk density	
Shipboard analysis	x
Shore-based analysis	x
Bulk density by 2-min. GRAPE	x

possible until Core 579A-9, when weather and sea-surface conditions permitted operation of the core-nose temperature probe. Subsequent measurements were satisfactory. All seven runs, made at every core from Cores 579A-9 through 579A-15, were successful. Two recorders, WHOI-01 and WHOI-4A, connected to battery packs TILT-2 and NTLT-2, respectively, were used alternately throughout the operation. The thermal gradient seems to be constant for the measured interval.

The constant thermal gradient combined with the thermal conductivity data, which were taken at 155 locations in Holes 579 and 579A, yielded a reliable heat flow value (see Horai and Von Herzen, this volume).

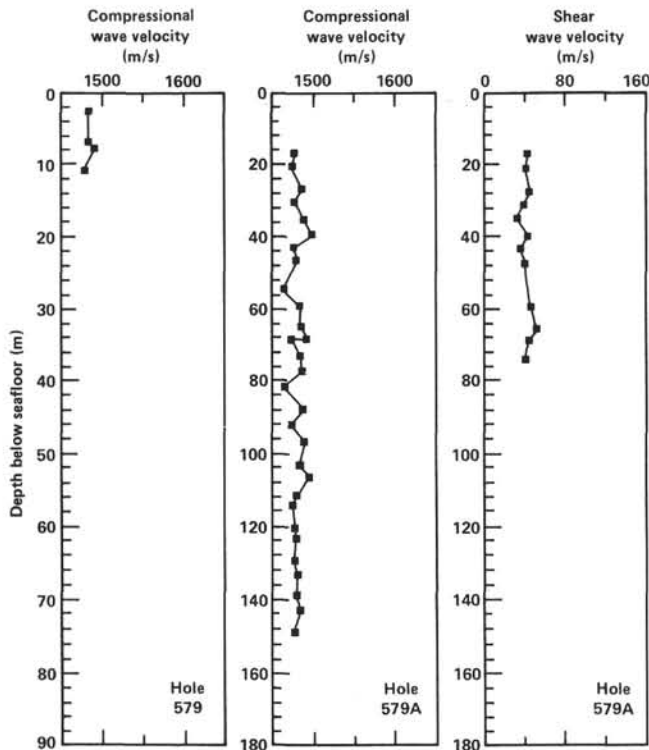


Figure 6. Plot of compressional and shear wave velocities versus sub-bottom depth at Site 579.

SUMMARY AND CONCLUSIONS

Some of the results of Site 579 are summarized in Figure 1. Only one major lithologic unit is recognized in this site. However, it is divided into three subunits as follows.

1. Subunit IA (0.0–60.0 m) is a siliceous clay, gray and gray green in color containing 15–30% quartz, 2–25% diatoms, and 0–15% radiolarians. Feldspar and disseminated volcanic ash are also present but usually in abundances of less than 5%. Approximately 45% clay forms the remainder of the sediment. Twenty-seven ash layers occur in this subunit, with thicknesses ranging from 2 to 19 cm. Also present are 83 thin, well indurated dark grayish green layers. These “green layers” are lithologically unlike the adjacent softer gray siliceous clay. Their origin is uncertain.

2. Subunit IB (60.0–102.5 m) is a clayey biosiliceous ooze. It contains 5–15% quartz, 4–30% diatoms, and 13–35% radiolarians. Disseminated volcanic glass forms less than 5%, and feldspar 2% or less, of the total sediment. The remainder (40%) is composed of clays. The subunit is differentiated from Subunits IA and IC by an increase in the percentage of radiolarians. Twenty-four ash layers and 126 indurated dark grayish green layers occur in this subunit.

3. Subunit IC (102.5–149.5 m) is a clayey diatom ooze, differentiated from the overlying subunit by a decrease in the radiolarian content. It contains 3–25% quartz, 25–60% diatoms, and 2–30% radiolarians. Disseminated volcanic ash and feldspar make up approximately 2–5% of the sediment. The remainder, about 38%, is composed of clays. This subunit contains 116 dark grayish green

indurated layers, and fewer ash layers (10) than the overlying subunits.

Figure 4 summarizes the paleomagnetism and biostratigraphy for this site. Although there were some problems in obtaining a coherent magnetic reversal record (intensities were only slightly above the noise level of the machine), an adequate record was obtained for at least the Quaternary and middle to late Pliocene. The interpretation of the paleomagnetism was supported by the radiolarian and diatom biostratigraphy. Biostratigraphic evidence suggests that early Pliocene sediments were penetrated at this site: Hole 579A terminated in the lower part of the *Nitzschia jouseae* diatom zone and the *Stichocorys peregrina* radiolarian zone.

The presence of numerous ash layers at Site 579 prompted us to plot numbers of ash layers/m.y. as has been done for other DSDP sites in the circum-Pacific. Figure 10 presents these data and shows that there is a general increase in ash layer density to the present day. This generally agrees with the results of Furuta and Arai (1980), who attribute this increase to plate motion rather than to episodic volcanicity.

The great volume of ash, contributed mainly from the Japanese Islands, together with the high productivity in this region, have contributed to a high sedimentation rate, particularly for the late Pliocene and Pleistocene. Figure 5 summarizes the relevant data from paleomagnetic determinations in an age–depth diagram. Rates as high as 40–45 m/m.y. were achieved in the Quaternary. Rates were lower, however, around the Pliocene/Pleistocene boundary, but were high again in the late Pliocene.

In spite of the numerous ash layers and semi-indurated green layers recovered at this site, it was difficult to pinpoint the source of the seismic reflections. This was partially due to the sea state when the site was occupied, resulting in frequent distorted bedding and flow-in. A second consideration, however, was the large number of distinct, but closely spaced reflectors in the upper 70 m of the hole. In spite of this, we feel that we can identify some ash layers as discrete reflectors. Interestingly, it appears that only the ash horizons serve as seismic reflectors; there is no evidence that the indurated green layers show up on the seismic records, in spite of the fact that spikes in the compressional wave velocity profile are produced by both the ash and the green layers. Typical v_p velocities are on the order of 1.6 km/s whereas the velocities in the green layers, although variable, range as high as 1.77 km/s. Other changes in sediment physical properties are likely due to changes in clay mineralogy.

The sea-state prevented us from making heat flow measurements in the upper part of Hole 579A. Observations began at 100 m and continued to 160 m, with the temperature data clearly showing a linear increase with depth.

The objectives at this site—to recover a detailed paleoceanographic record of the subtropical–subarctic transition zone for the late Cenozoic, to establish a high resolution, multitaxa stratigraphy for the late Cenozoic northwest Pacific, to determine the time of onset of significant biosiliceous accumulation, and to determine the late Cenozoic history of eolian input for comparison

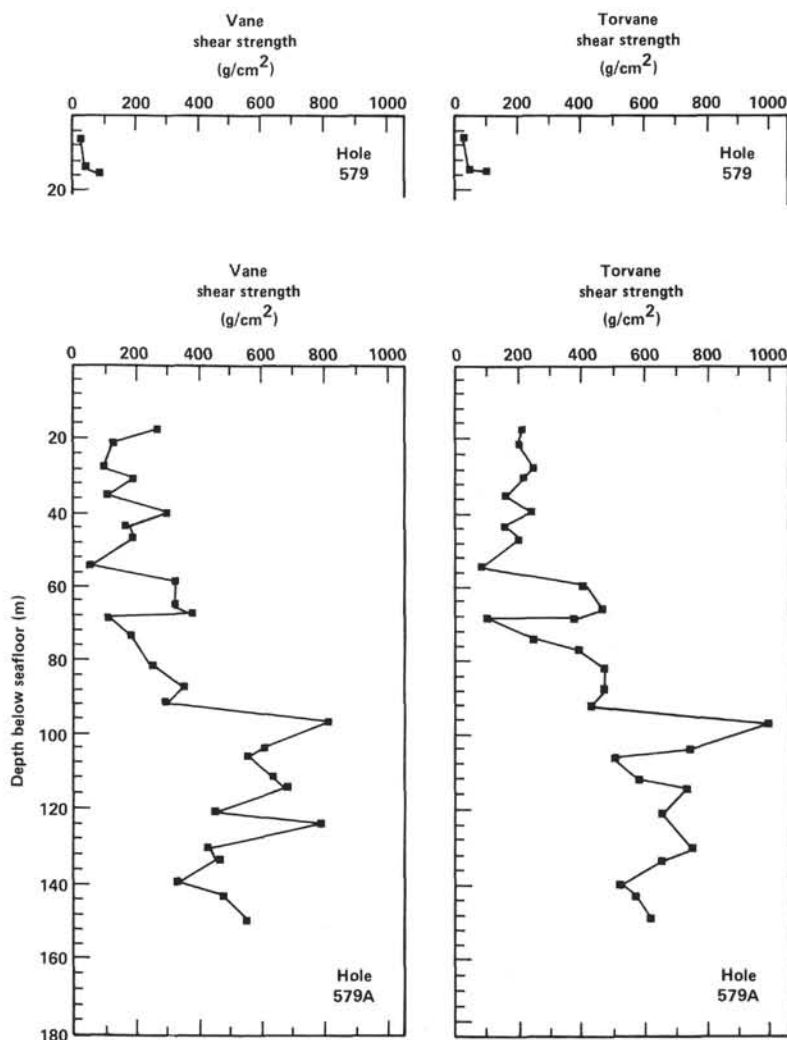


Figure 7. Plot of shear strength versus sub-bottom depth at Site 579.

with the history of north-south migration of the subarctic front—were largely achieved. Further, we obtained an excellent record of late Cenozoic ash falls on the northwest Pacific to complement the record from Site 578.

Because of time limitations coupled with increasingly poor penetration, we were unable to reach the transition from biosiliceous sediments into the underlying red clay as we had at Site 578.

REFERENCES

- Berggren, W. A., Kent, D. V., and Flynn, J. J., in press. Paleogene geochronology and chronostratigraphy. In Snelling, N. J. (Ed.), *Geochronology and the Geological Record*. Geol. Soc. London Spec. Pap.
- Boyce, R. E., 1976a. Definitions and laboratory techniques of compressional and sound velocity parameters and wet-water content, wet-bulk density, and porosity parameters by gravimetric and gamma ray attenuation techniques. In Schlanger, S. O., Jackson, E. D., et al., *Init. Repts. DSDP*, 33: Washington (U.S. Govt. Printing Office), 931-958.
- , 1976b. Deep Sea Drilling Project procedures for shear strength measurements of clayey sediment using modified Wykeham Farrance Laboratory Vane Apparatus. In Barker, P., Dalziel, I. W. D., et al., *Init. Repts. DSDP*, 36: Washington (U.S. Govt. Printing Office), 1059-1068.
- Burckle, L. H., 1972. Late Cenozoic planktonic diatom zones from the eastern equatorial Pacific. *Nova Hedwigia Beih.*, 39: 217-246.
- Foreman, H. P., 1973. Radiolaria from DSDP Leg 20. In Heezen, B. C., MacGregor, I. D., et al., *Init. Repts. DSDP*, 20: Washington (U.S. Govt. Printing Office), 249-305.
- , 1975. Radiolaria from the North Pacific, Deep Sea Drilling Project, Leg 32. In Larson, R. L., Moberly, R., et al., *Init. Repts. DSDP*, 32: Washington (U.S. Govt. Printing Office), 579-701.
- Furuta, T., and Arai, F., 1980. Petrographic properties of tephros, Leg 56, Deep Sea Drilling Project. In Scientific Party, *Init. Repts. DSDP*, 56, 57, Pt. 2: Washington (U.S. Govt. Printing Office), 1043-1048.
- Hays, J. D., 1970. Stratigraphy and evolutionary trends of Radiolaria in North Pacific deep-sea sediments. In Hays, J. D. (Ed.), *Geological Investigations of the North Pacific*. Mem. Geol. Soc. Am., 126:185-218.
- Koizumi, I., 1973. The late Cenozoic diatoms of Sites 183-193, Leg 19, Deep Sea Drilling Project. In Creager, J. S., Scholl, D. W., et al., *Init. Repts. DSDP*, 19: Washington (U.S. Govt. Printing Office), 805-855.
- Riedel, W. R., and Sanfilippo, A., 1970. Radiolaria, Leg 4, Deep Sea Drilling Project. In Bader, R. G., Gerard, R. D., et al., *Init. Repts. DSDP*, 4: Washington (U.S. Govt. Printing Office), 503-575.

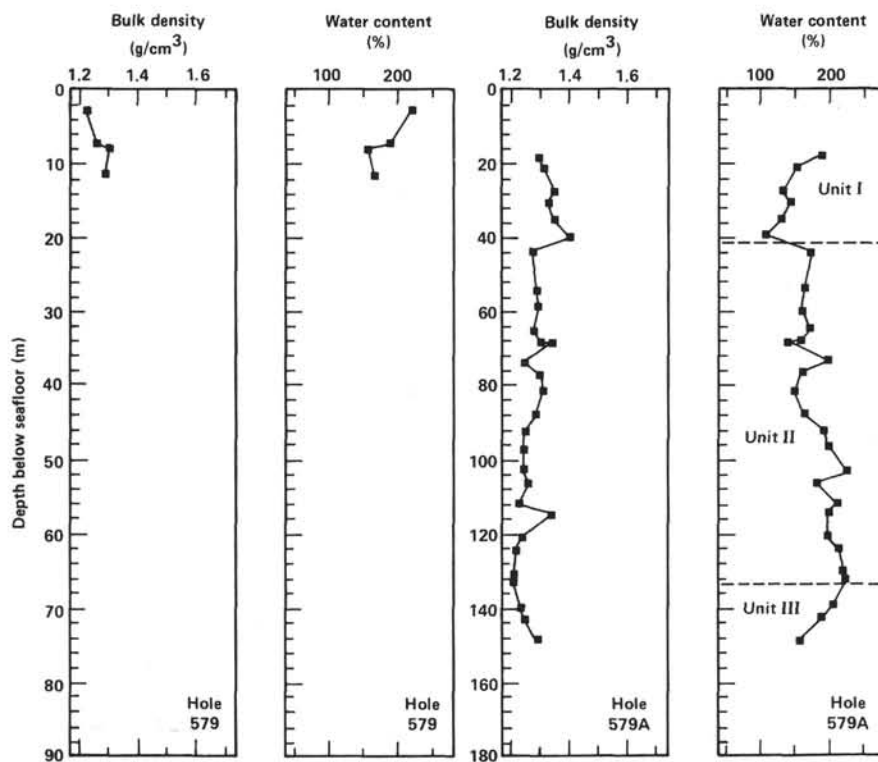


Figure 8. Profiles of saturated bulk density and water content versus sub-bottom depth at Site 579. Physical properties Units I, II and III are discussed in the text.

Table 5. Inorganic geochemical measurements made at Site 579.

Sample	pH	Alkalinity (mEq/l)	Salinity (‰)	Calcium (mM)	Magnesium (mM)	Chlorinity (‰)
IAPSO	8.62	2.45	35.2	10.55	53.99	19.38
SSW	8.74	2.36	34.9	10.37	53.03	19.07
579-2-5, 140-150 cm	8.37	5.13	35.2	10.77	50.71	19.34
579A-5-5, 140-150 cm	8.28	5.87	36.3	11.51	48.71	19.54
579A-8-5, 140-150 cm	8.42	5.73	35.2	11.92	47.52	19.41
579A-11-4, 140-150 cm	8.54	5.40	34.9	12.51	47.17	19.51
579A-14-4, 140-150 cm	8.27	4.85	34.9	12.85	45.63	19.44

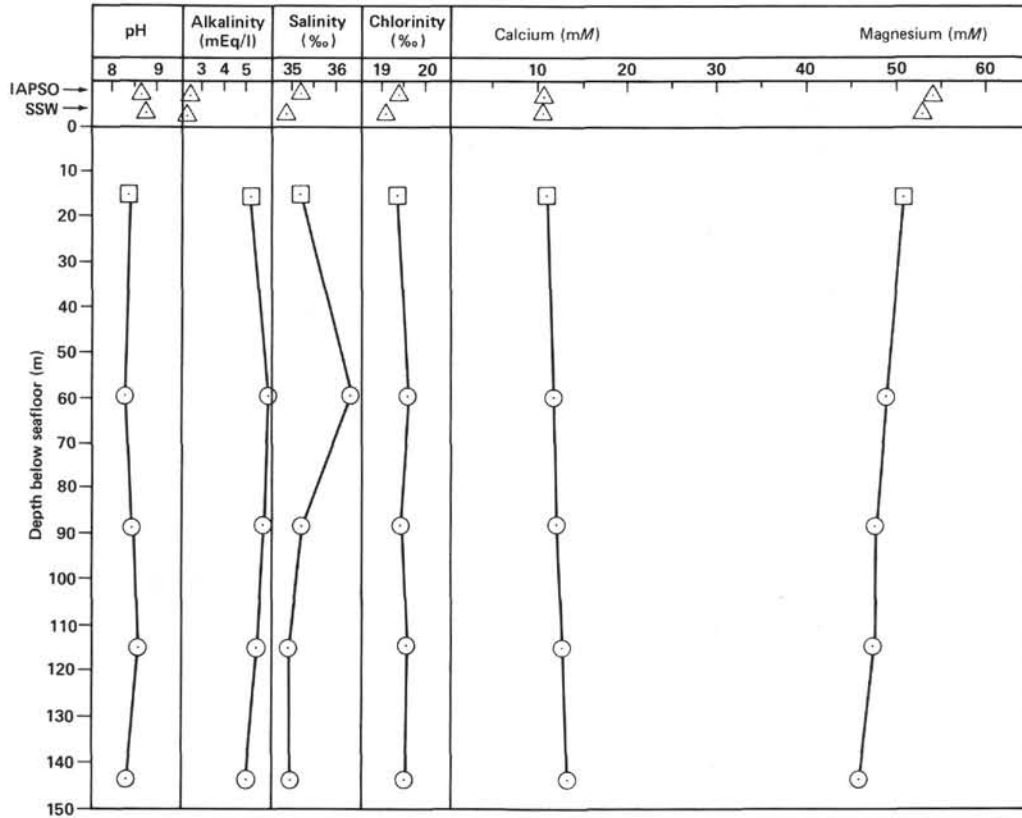


Figure 9. Profiles of pH, alkalinity, salinity (‰), chlorinity (‰), calcium (mM), and magnesium (mM) versus sub-bottom depth from interstitial water samples analyzed at Site 579. Symbols are as follows: Δ = IAPSO and SSW standards; \square = samples from Hole 579; \odot = samples from Hole 579A.

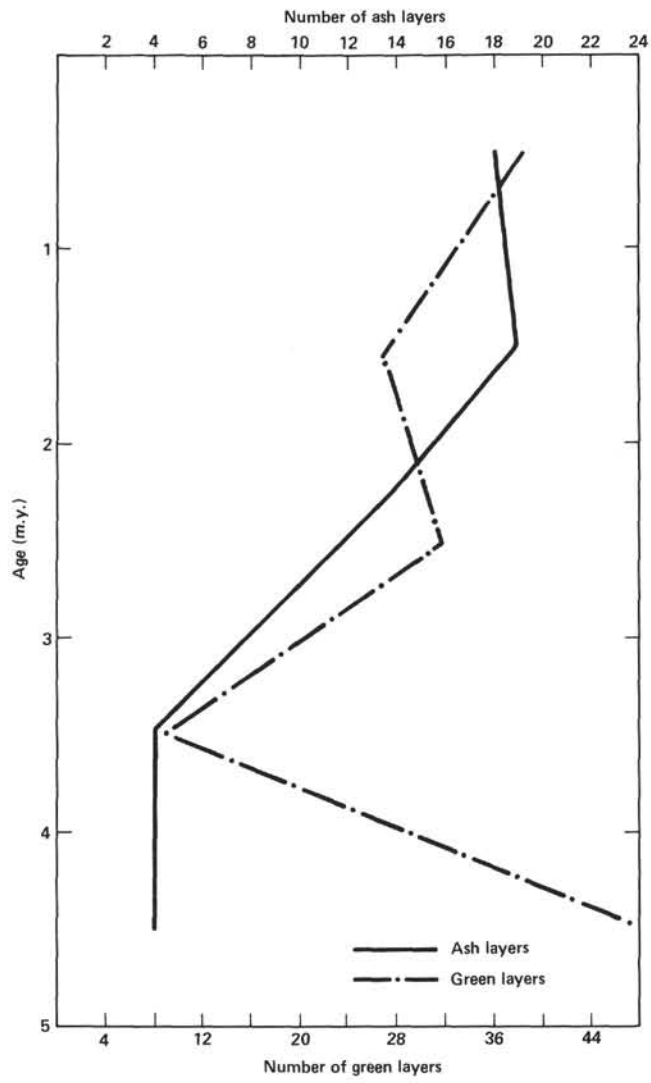
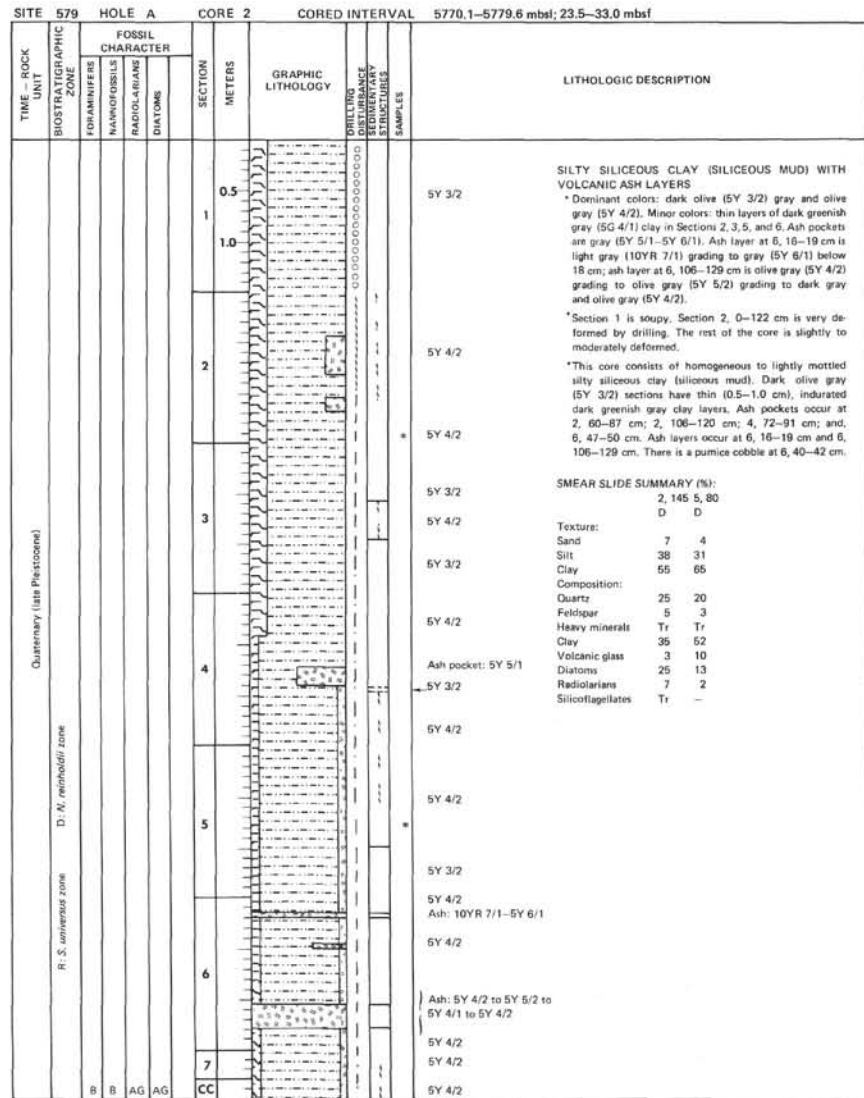
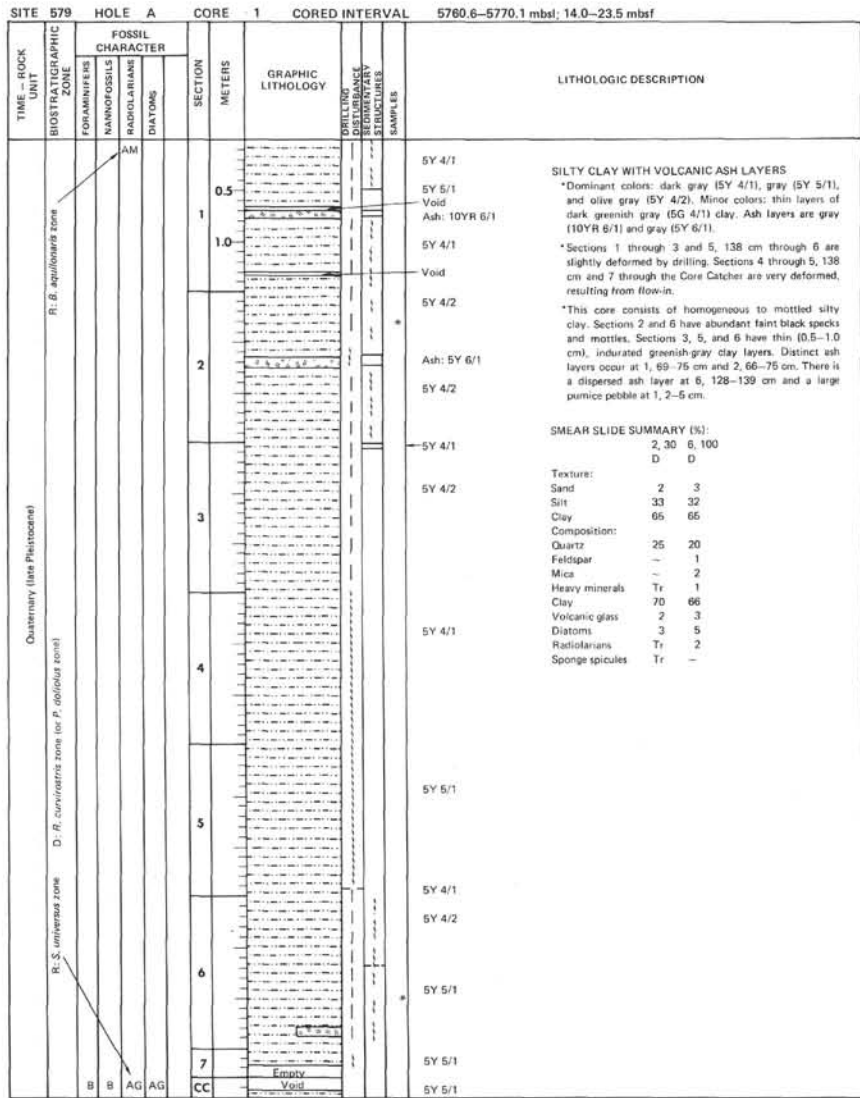
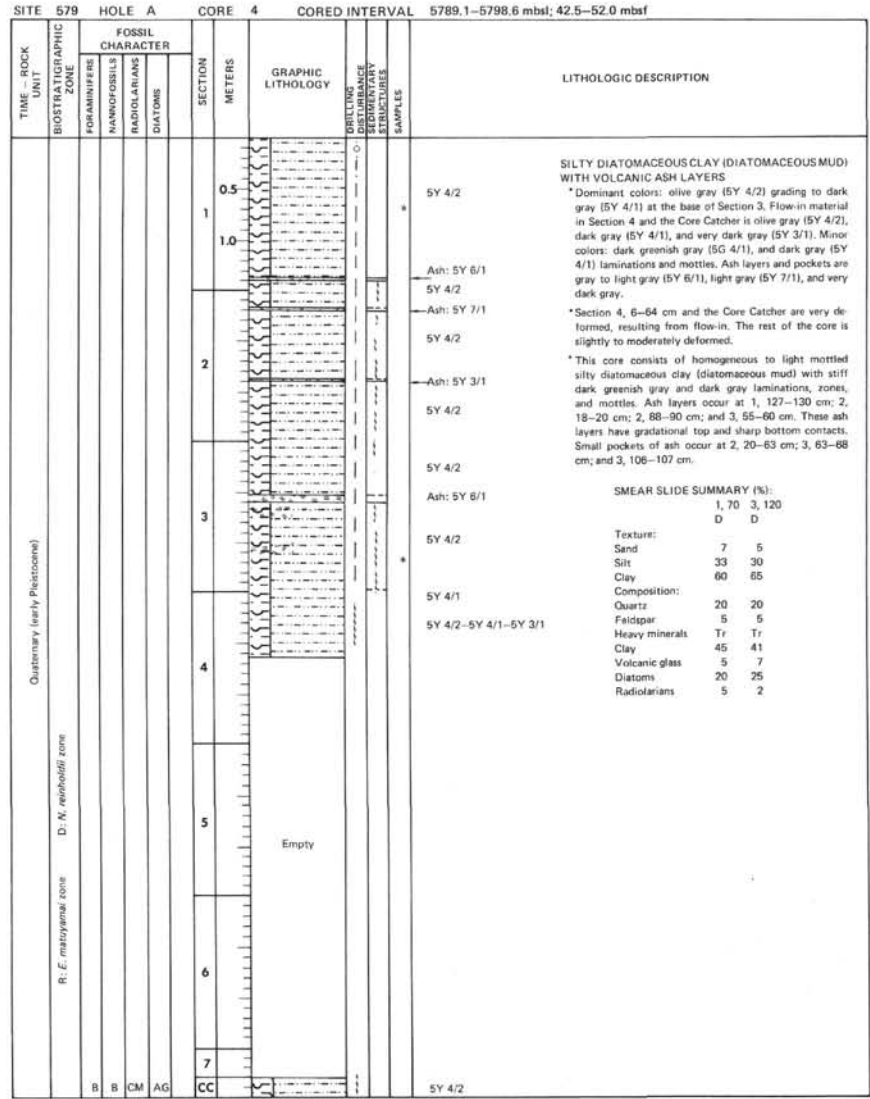
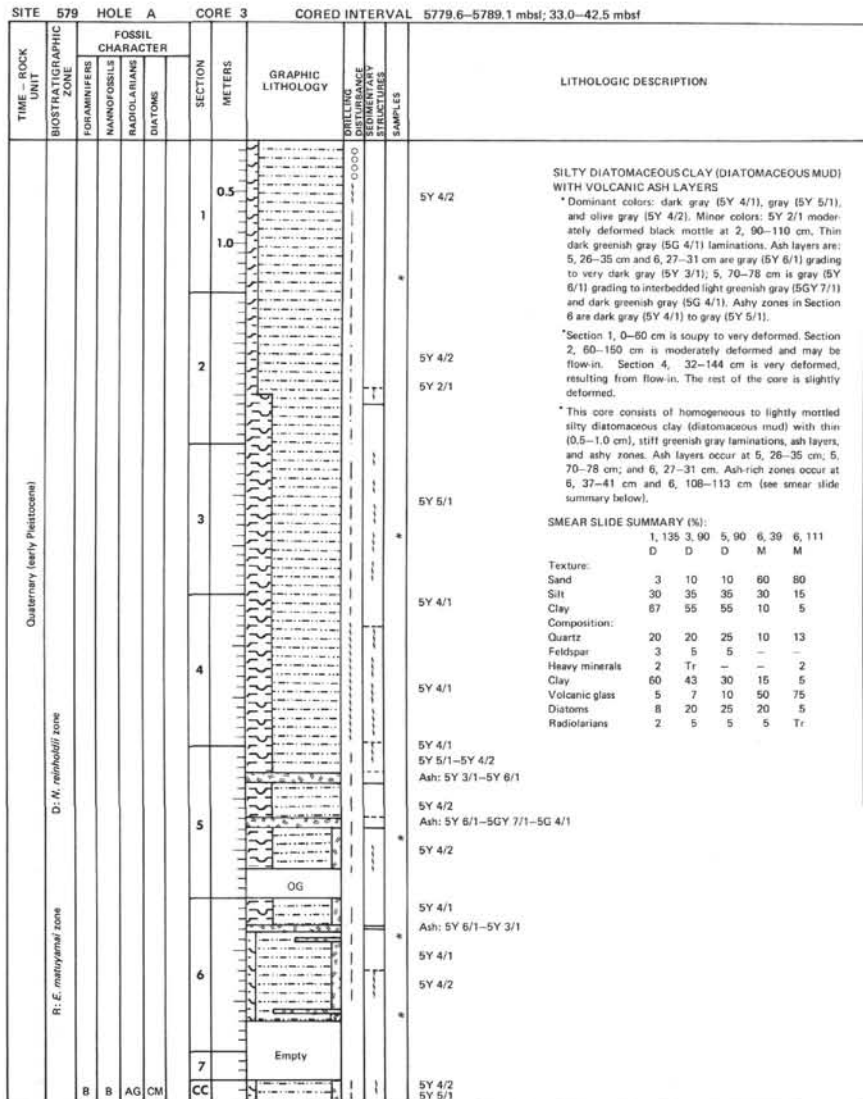
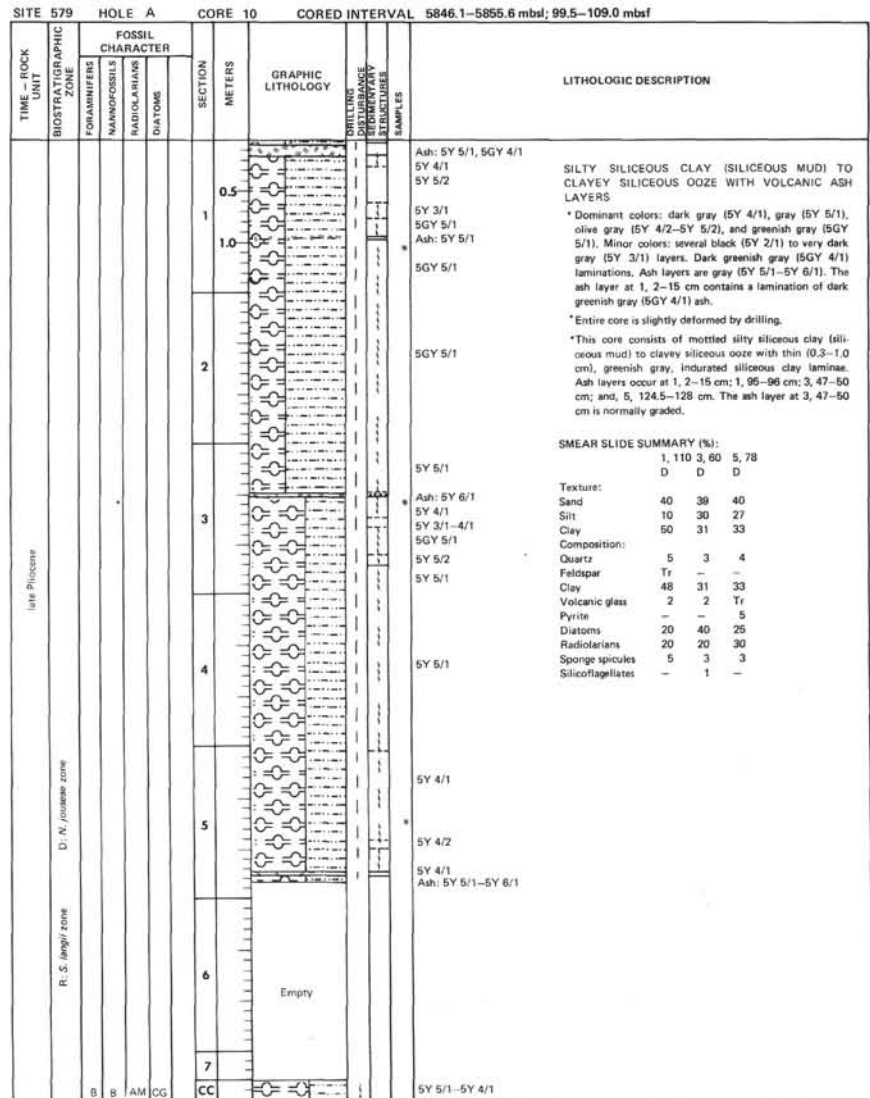
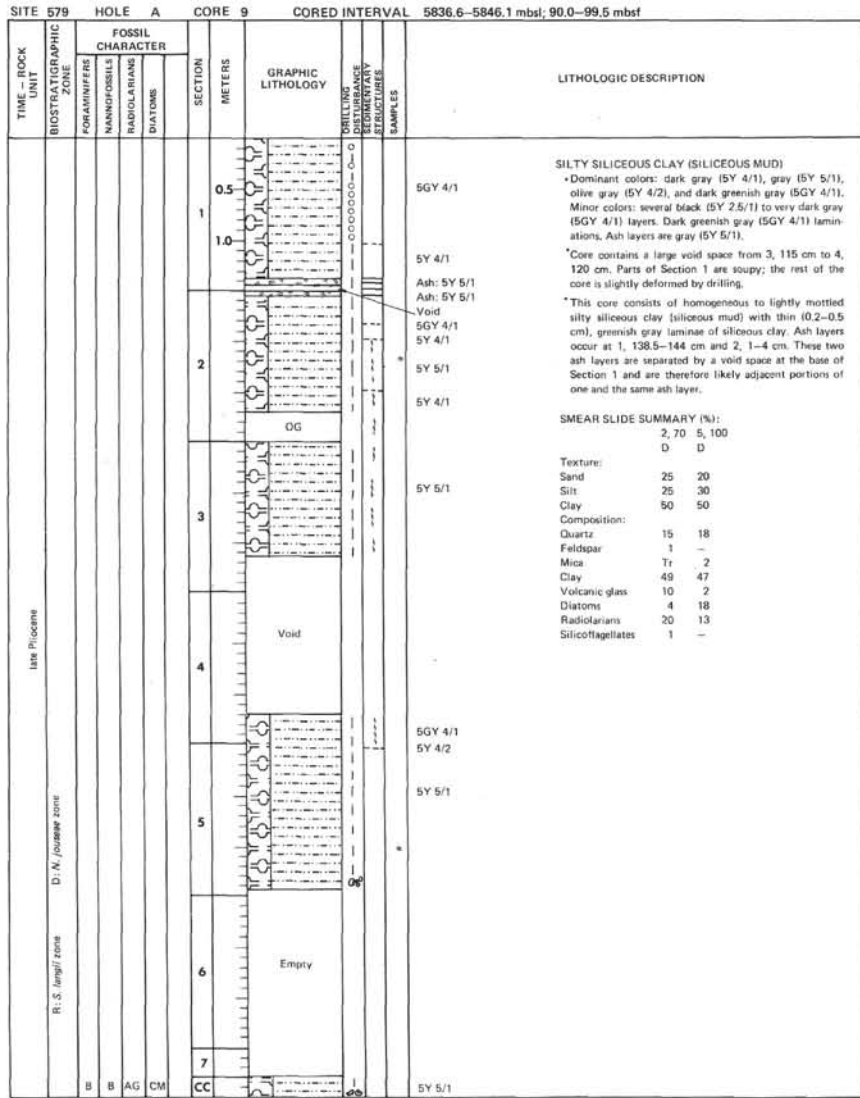
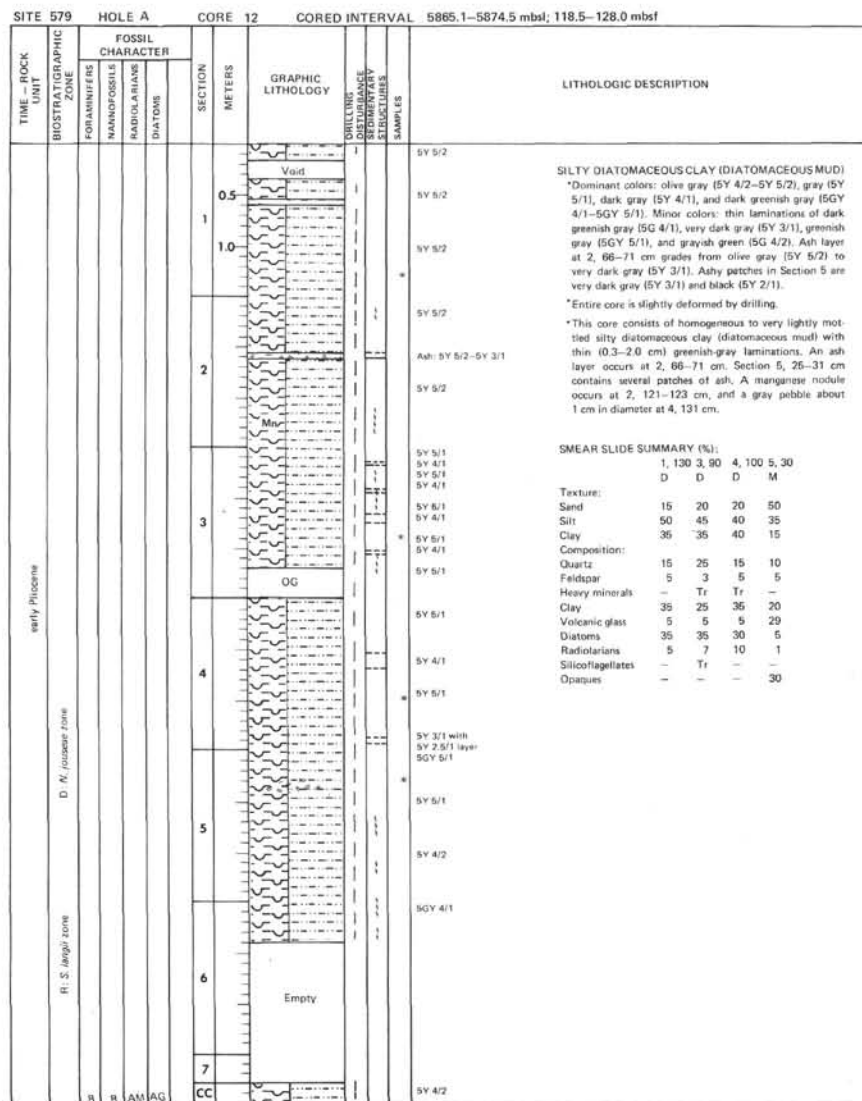
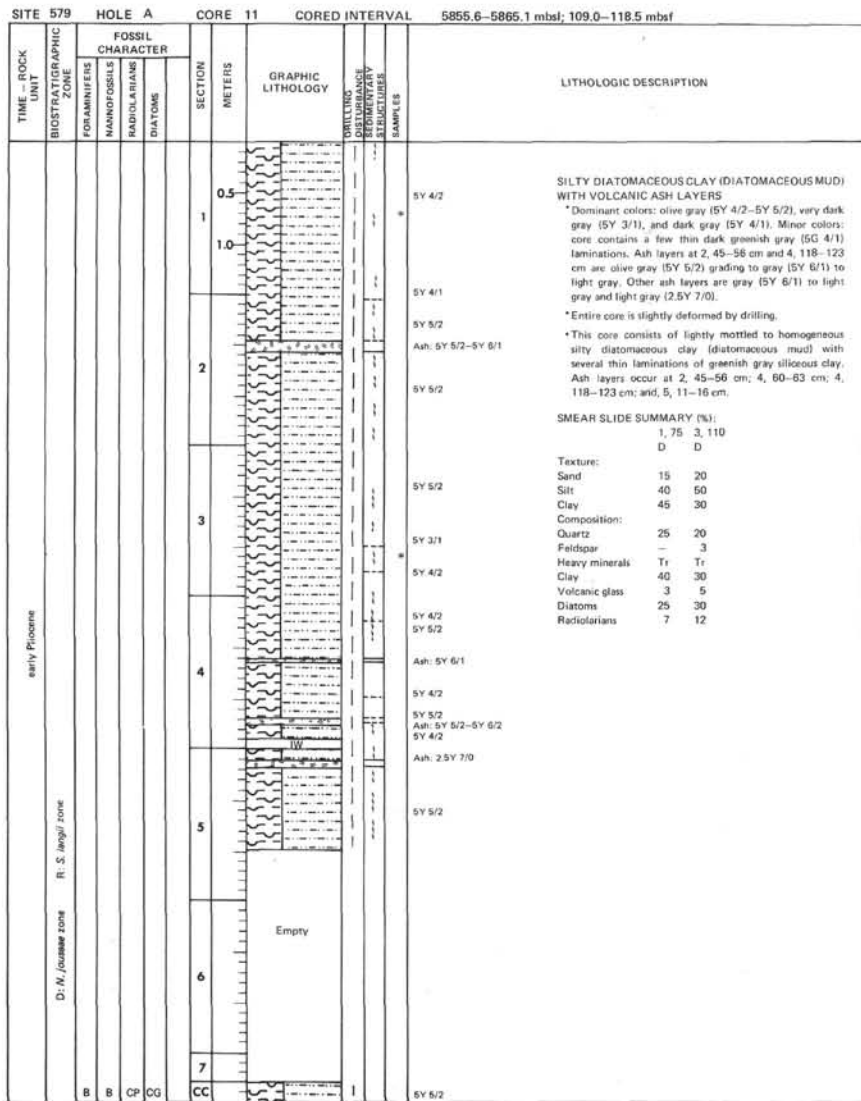


Figure 10. Plot of numbers of ash layers and indurated green layers/m.y. at Site 579.









SITE 579 HOLE A CORE 15 CORED INTERVAL 5893.6-5896.1 mbsl; 147.0-149.5 mbsf

TIME - ROCK UNIT	BIOSTRATIGRAPHIC ZONE	FOSSIL CHARACTER			SECTION METERS	GRAPHIC LITHOLOGY	DIRECTION OF SEDIMENTARY TRENDS	CORRECTION SAMPLES	LITHOLOGIC DESCRIPTION																												
		FORAMINIFERS	NANNOFOSSILS	RADIOLARIANS						DIATOMS																											
ashy Pliocene	D. N. /oussae zone				0.5				<p>CLAYEY DIATOM OOZE</p> <p>*Dominant colors: greenish gray (5GY 5/1), dark greenish gray (5GY 4/1), and dark gray (5Y 4/1). Minor colors: dark greenish gray (5G 4/1) zones and laminations in Section 2, 60-88 cm. Ash in the Core Catcher is gray (5Y 6/1) to light gray.</p> <p>*Section 1, 0-71 cm is soupy to very deformed. The rest of the core is slightly deformed by drilling.</p> <p>*This core consists of clayey diatom ooze. The greenish gray portions of Section 1 and Section 2, 0-60 cm are homogeneous. The dark gray portion at 2, 60-88 cm is mottled and contains greenish gray laminations. An ash layer occurs in the Core Catcher at 46-49 cm.</p> <p>SMEAR SLIDE SUMMARY (%):</p> <table border="0"> <tr><td></td><td>1, 110</td></tr> <tr><td>D</td><td></td></tr> <tr><td>Texture:</td><td></td></tr> <tr><td>Sand</td><td>10</td></tr> <tr><td>Silt</td><td>50</td></tr> <tr><td>Clay</td><td>40</td></tr> <tr><td>Composition:</td><td></td></tr> <tr><td>Quartz</td><td>7</td></tr> <tr><td>Feldspar</td><td>3</td></tr> <tr><td>Clay</td><td>27</td></tr> <tr><td>Volcanic glass</td><td>10</td></tr> <tr><td>Diatoms</td><td>45</td></tr> <tr><td>Radiolarians</td><td>5</td></tr> <tr><td>Silicoflagellates</td><td>3</td></tr> </table>		1, 110	D		Texture:		Sand	10	Silt	50	Clay	40	Composition:		Quartz	7	Feldspar	3	Clay	27	Volcanic glass	10	Diatoms	45	Radiolarians	5	Silicoflagellates	3
			1, 110																																		
		D																																			
		Texture:																																			
		Sand	10																																		
		Silt	50																																		
		Clay	40																																		
Composition:																																					
Quartz	7																																				
Feldspar	3																																				
Clay	27																																				
Volcanic glass	10																																				
Diatoms	45																																				
Radiolarians	5																																				
Silicoflagellates	3																																				
				1.0																																	
				2																																	
				3	Empty																																
				4																																	
				5																																	
				6																																	
				7																																	
B		AM	AM	CC				5GY 4/1 Ash: 5Y 6/1																													

